Egy. J. Pure & Appl. Sci. 2016; 54(4):31-36

Egyptian Journal of Pure and Applied Science

Photocatalytic degradation of Methyl orange and Rhodamine B over TiO_2 prepared by sol-gel method: parametric study

Mohamed A. Ahmed, Michel F. Abdel-Messih, Mai. H. Abdel-Khalek*, Mohamed F. El-Shahat

Chemistry Department, Faculty of Science, Ain Shams University, Cairo, Egypt

ARTICLE INFO

Article history:
Received 01 November 2016
Accepted 17 December 2016

Keywords:
TiO_2;
Photocatalysis;
Sol-gel;
Methyl orange;
Rhodamine B.

ABSTRACT

TiO_2 was synthesized by a sol-gel method using chitosan as a structure-directing agent. The prepared nanoparticle was characterized using XRD, FESEM and HRTEM techniques. Nanoparticles prepared in this work exhibited spherical shape with particle size ranged 8-13nm. Parameters affect the photocatalytic degradation as catalyst dosage, initial dye concentration and pH examined for methyl orange (MO) and Rhodamine B (RhB) dyes. It was found that the degradation process strongly depends on these parameters. The reusability of the TiO_2 is investigated during five cycle experiments, the activity of the catalyst showed good activity at the cycles which indicates that the TiO_2 can be used repeatedly.

Introduction

Lately, the ubiquity of pollutants shows a serious risk to the environment. For instance, 15% of the total dye is discharged into water via industrial wastewater [1].

Dyes can generate dangerous by-products through oxidation, hydrolysis or other chemical reactions taking place in the wastewater. Methyl Orange (MO) and Rhodamine B (RhB) are intensively used in dyeing and printing textiles, their release into water represents a potential hazard to the environment [2-4]. Photocatalysis process has received a great interest in solving water treatment problems owing to its great ability for destruction of pollutants. Titanium dioxide (TiO_2) has become one of the most used semiconductors because of its high redox ability, high efficiency, low cost, stability, and nontoxicity [5-12].

TiO_2 mainly exists in three crystalline forms - Anatase, Rutile and Brookite [3], in which brookite structure is less important in the field of photocatalysis because it is very difficult to obtain it in the pure form, two different crystal structures of TiO_2, rutile and anatase are commonly used in photocatalysis and the latter has higher photocatalytic activity than the former probably because of its higher conduction band energy. However, rutile has lower activity due to its high preparation temperature, in which agglomeration of the particles can occur, leading to lower surface area and consequently increment of particle size. Upon irradiation of TiO_2 with light energy greater than its bandgap, the electron from the valence band of TiO_2 will be promoted to conduction band leaving a hole in valence band, the photogenerated holes and electrons react with oxygen and water molecules yielding reactive hydroxyl radicals ($OH^{\bullet}$), which destruct the hazardous pollutants [5].

Sol-gel method has been used to prepare photocatalysts based on a hydrolysis reaction of metallic alkoxides followed by a polycondensation. Since this method is a solution process, it allows tailoring structural characteristics such as compositional homogeneity, grain size, particle morphology and porosity [13-19]. TiO_2 prepared by sol–gel method using chitosan as a template was recently reported for photocatalytic degradation of methylene blue [20], the aim of this work is to prepare TiO_2 photocatalyst by sol–gel method using chitosan and to study its photocatalytic activity for degradation of methyl orange (MO) and Rhodamine B (RhB), the photocatalytic degradation was studied by various parameters such as catalyst dosage, initial dye concentration, and pH. Furthermore, the reusability of the photocatalyst was investigated to provide an insight on catalyst stability.

Materials and methods

Materials

Titanium isopropoxide, Chitosan, Methyl orange dye, Rhodamine B dye and Isopropanol are purchased from Sigma-Aldrich with purity=99%. All these chemicals were used without further purification.

Catalyst preparation

TiO_2 photocatalyst was prepared by a sol–gel process [20], 5 ml of titanium tetraisopropoxide was dissolved in 50 ml of isopropanol then adding chitosan dissolved in acetic acid as structure-directing agent, a few drops of water

* Corresponding author.
E-mail address: maihussein65@yahoo.com

was added with vigorous stirring for 2 h, the sol was aged for 48 h form gel. The powder was obtained after drying, grinding and calcination at 500°C for 2h.

Determination of pH_{pzc}

The pH at the point of zero charge (pH_{pzc}) for the TiO_2 in a solid to solution ratio of 1:250 was determined by the batch equilibration technique. Sodium chloride solution (0.1 mol/L NaCl) was used as an inert electrolyte. Initial pH values ($pH_{initial}$) of the NaCl solutions were adjusted from 1 to 12 by the addition of 0.1mol/L HCl or NaOH. TiO_2 (0.1 g) was added into 25 mL of 0.1mol/L NaCl solution. The suspension mixture (1:250) was allowed to equilibrate for 24 h maintained at room temperature. Then the pH values (pH_{final}) were measured [21].

Characterization and analysis

X-ray diffraction (XRD) patterns were carried out by X'PERT MPD diffractometer using Cu ($K\alpha_1/K\alpha_2$) radiation. Crystallite sizes were calculated from the line broadening of the main X-ray diffraction peaks by using the Scherrer equation.

Surface morphology was carried out by Scanning electron microscopy obtained in a JEOL - JSM-5410 instrument.

High Resolution Transmission Electron Microscopy (HRTEM) was performed on a JEOL 2000FX instrument.

Photocatalytic reaction

The evaluation of the photocatalytic activity of the catalyst was performed by using the MO or RhB solution as a pollutant. The dye solution and the catalyst were placed in a pyrex discontinuous batch reactor illuminated through a UV radiation (spectro line lamp 40 W) with a main line in the UVA range at 365 nm. Before illumination, the suspensions were magnetically stirred in the dark for 60 min to establish the adsorption/desorption equilibrium of the dye. At given irradiation time intervals samples were taken from the suspension and immediately centrifuged. The absorption spectrum was analyzed by Shimadzu UV–visible spectrophotometer (model-1601). The maximum absorbance of the dye solution was used to determine the concentration of the collected aliquots.

The decolorization (%) was calculated from the following equation:

$$\text{decolorization (\%)} = [(C_o - C_t)/C_o] \times 100$$

Where C_o is initial concentration (mole/L), C_t is the concentration of the dye at various interval times (mole/L).

Results and discussion

Structural and chemical characterization.

Crystalline phase composition and degree of crystallinity were studied by X-ray diffraction. **Fig. 1** shows the XRD patterns for TiO_2, which characterized with sharp crystalline peaks at 2θ =25.3, 36.9, 37.7, 38.5, 48, 51.9, 53.8, 55.1, 62.6, 68.7, and 75 (JCPDS file No: 71- 1167). It is obvious to notice the disappearance of rutile diffraction peaks indicating that chitosan motivates the formation of anatase phase by well dispersing between titania crystallites and preventing agglomeration during the progress of calcinations. The average crystallite size was estimated by the Scherrer equation (eq.1), Anatase crystalline size for prepared TiO_2 was 14.6 nm.

$$D = K\lambda/\beta\cos\theta \quad \textbf{(1)}$$

Where D is the crystal size of the catalyst, λ the X-ray wavelength (1.54 Å), β the full width at half maximum (FWHM) of the catalyst (radian), K = 0.89 and ɵ is the diffraction angle.

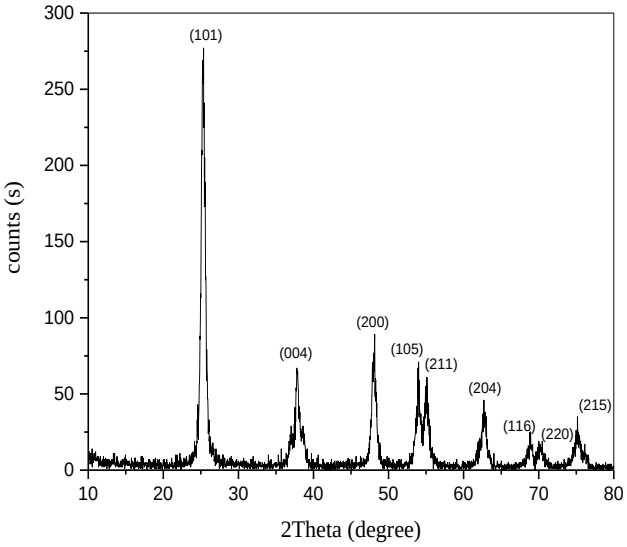

Fig (1): X-ray diffraction of TiO_2

The scanning electron microscopic image of TiO_2 is shown in **Fig. 2 (A)**. The image shows that the particles are spherical in nature. Particles in nano size range are clearly observed from the HRTEM images as shown in **Fig. 2 (B & C)**. It can be noted from the images that the particles are spherical in shape, these results are in good agreement with the results of SEM. SAED patterns indicate the existence of several diffractions rings revealing the high crystallinity of the samples **Fig. 2 (D)**.

Photocatalytic activity

Photocatalytic activity was evaluated by measuring the decrease in absorbance of MO and RhB. Decolorization rate for RhB is higher than MO (**Fig. 3**) owing to adsorption of RhB on titania surface with a higher percentage than MO as shown in **Fig. 3** (inset). The high adsorption of RhB compared to MO TiO_2 may be improve the transportation of RhB molecules to the vicinity of photocatalytic site, thereby facilitated its photocatalytic degradation.

Catalyst dose

The effect of catalyst dose on decolorization rate was studied by varying catalyst concentration. It is found that the decolorization of MO solution increased from 11.09% to 48.22% with the increase of catalyst concentration in a range from 0.75 g/L to 2 g/L (**Fig. 4**), while for RhB solution increased from 43% to 72% with the increase of catalyst concentration in a range from 0.5 g/L to 1 g/L (**Fig. 5**). This can be explained in terms of

availability of the active sites on the catalyst surface as the total active surface area increases with the catalyst dosage, The decolorization rate decreased to 33% and 66% with further increase of catalyst dosage for MO and RhB respectively, which reveals that the light has been scattered by the higher catalyst dosage [22]. Catalyst dose 2 g/L and 1g/L were selected as the optimal TiO_2 dosage for MO and RhB respectively.

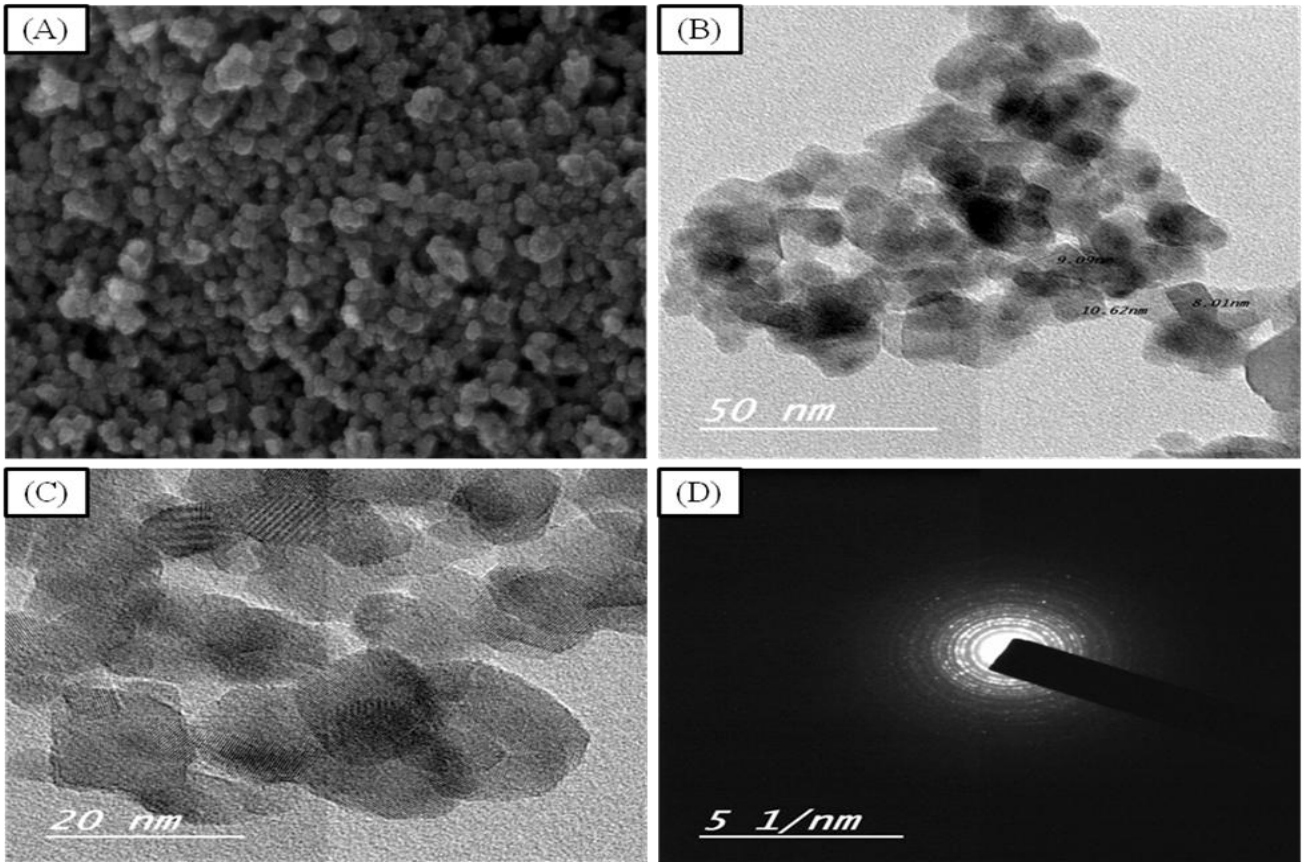

Fig (2): (**A**) FESEM, (**B and C**) HRTEM, (**D**) SAED image.

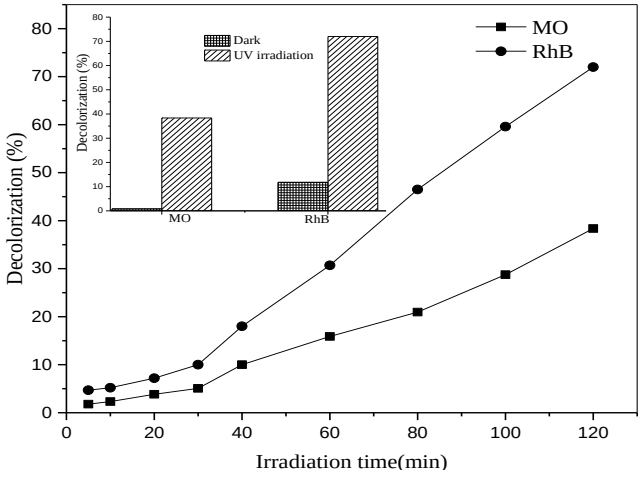

Fig (3): Photodegradation of MO and RhB over TiO_2. Experimental conditions: C_o = 3X10^{-5} mole/L for MO or C_o=1x10^{-5} mole/L for RhB, catalyst dosage = 1 g/L, pH=7, 365 nm UV lamp.

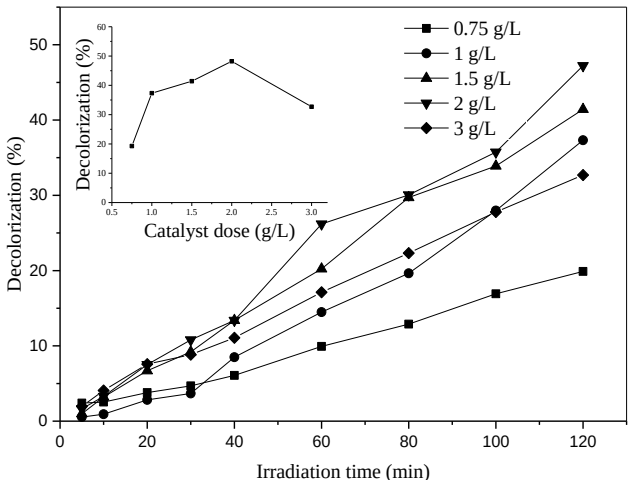

Fig (4): Effect of catalyst dosage on photocatalytic degradation of MO over TiO_2, Experimental conditions: C_o =3x 10^{-5} mole/L, pH=7, 365 nm UV lamp.

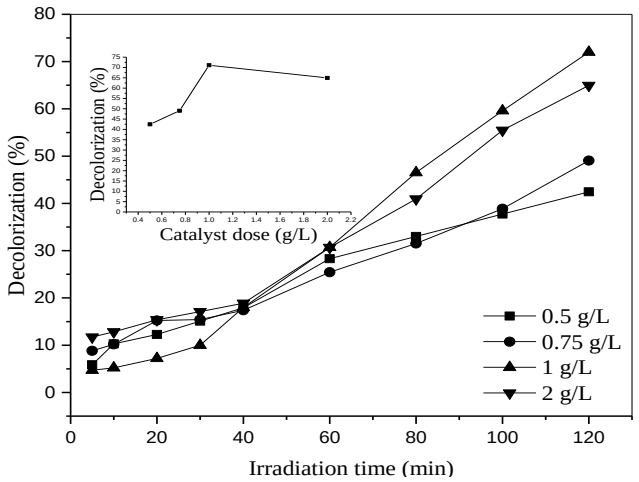

Fig (5): Effect of catalyst dosage on photocatalytic degradation of RhB over TiO_2, Experimental conditions: C_o =1x10^{-5} mole/L, pH=7, 365 nm UV lamp.

Initial dye concentration

The effect of initial dye concentration was studied by varying concentration of the dye. The degradation efficiency decreases with increasing the dye concentration as shown in **Fig. 6** and **Fig. 7**, this attributed to a reduction of photogenerated radicals on the catalyst surface since the active sites are covered by higher dye concentration [23]. Another possible reason is that portion of UV light can be absorbed by the dye molecules rather than the TiO_2 particles and thus the photocatalytic activity might be retarded, initial dye concentration less than 4x10^{-5} mol/L and 3x10^{-5} mol/L were selected as a suitable concentration for MO and RhB photodegradation, respectively.

pH

pH is an important parameter that affects the photocatalytic process. The photocatalytic decolorization was determined at five different pH levels 3, 5, 7, 9, and 11. The pH was adjusted using NaOH and HCl. The pH_{pzc} of TiO_2 was found 6.7 as shown in **Fig. 8**. At pH lower than the pH_{pzc}, the surface of TiO_2 is positively charged while for pH higher than the pH_{pzc}, the surface becomes negatively charged [23,24], according to the following equilibria:

$pH < pH_{pzc}$: $Ti–OH + H^+ \Leftrightarrow TiOH_2^+$

$pH > pH_{pzc}$: $Ti–OH + OH^- \Leftrightarrow TiO^- + H_2O$

MO dye exhibits high decolorization at acidic condition due to the electrostatic attraction between the negatively charged dye and positively charged TiO_2 surface ($TiOH_2^+$) (**Fig. 9**). We notice also a higher methyl orange adsorption at acidic pH compared to alkaline pH, while less decolorization obtained at alkaline condition due to electrostatic repulsions between negatively charged of the anionic sulfonated dye and negatively charged TiO_2 surface (TiO^-) groups on the semiconductor surface. Thus, MO molecules are scarcely adsorbed [25]. RhB dye exhibits high decolorization at a wide range of pH (**Fig. 9**) for the following reasons, RhB a zwitterionic dye, which has been found to be adsorbed at alkaline pH due to the electrostatic attraction between dye molecule which exists as cation at this pH level and negatively charged TiO_2 surface, In acidic medium the RhB ions are of cationic and monomericmolecular form, which could be easily diffused into the sites of the TiO_2 [26] (**Fig. 10**).

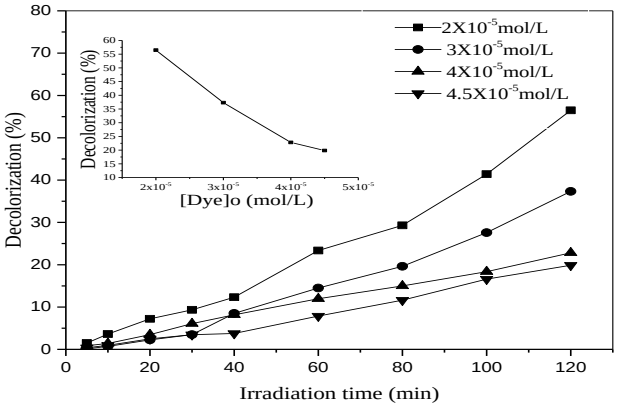

Fig (6): Effect of MO initial concentration on photocatalytic degradation over TiO_2. Experimental conditions: catalyst dosage = 1 g/L, pH=7, 365 nm UV lamp.

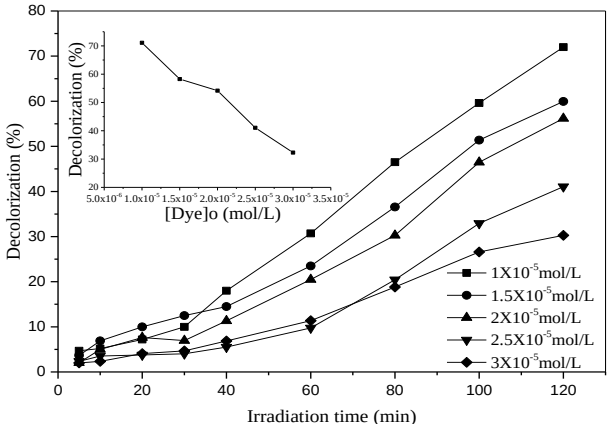

Fig (7): Effect of RhB initial concentration on photocatalytic degradation over TiO_2. Experimental conditions: catalyst dosage = 1 g/L, pH=7, 365 nm UV lamp.

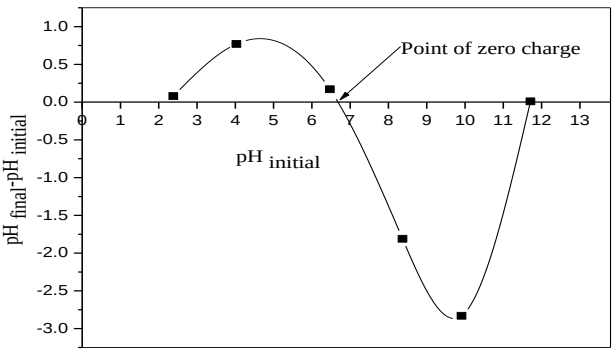

Fig (8): Plot of ($pH_{initial}$) versus (pH_{final} - $pH_{initial}$) for TiO_2.

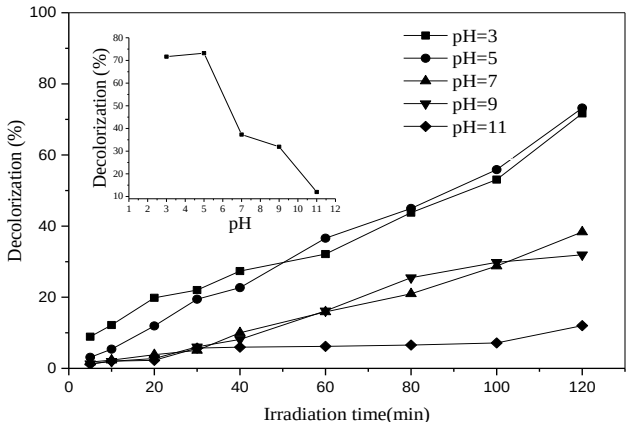

Fig (9): Effect of pH on photocatalytic degradation of MO over TiO_2. Experimental conditions: C_o = $3x10^{-5}$ mole/L, catalyst dosage = 1 g/L, 365 nm UV lamp.

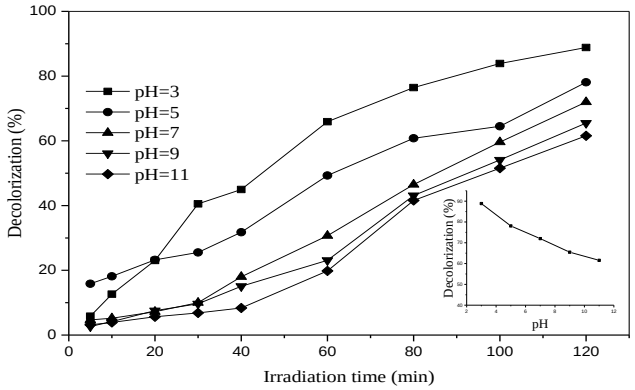

Fig (10): Effect of pH on photocatalytic degradation of RhB over TiO_2. Experimental conditions: C_o = $1x10^{-5}$ mole/L, catalyst dosage = 1 g/L, 365 nm UV lamp.

Reusability

Reusability of the photocatalyst is a key for the stability and the real application of the prepared sample, the decolorization efficiency of MO and RhB over TiO_2 remains almost without changes after five cycles (**Fig. 11**) that indicates the efficiency of the used method in the photocatalyst synthesis.

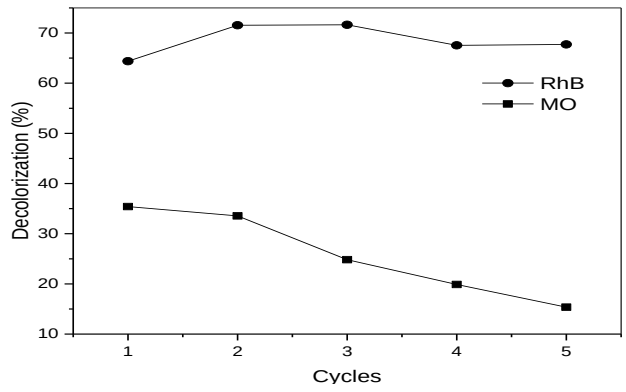

Fig (11): Reusability of MO and RhB over TiO_2, Experimental conditions: C_o = $3x10^{-5}$ mole/L for MO or C_o=$1x10^{-5}$ mole/L for RhB, catalyst dosage = 1 g/L, pH=7, 365 nm UV lamp.

Conclusions

TiO_2 nanoparticle was prepared by the Sol-gel method using chitosan as a template exhibited pure anatase phase, the prepared photocatalyst applied for the degradation of MO and RhB with successful photocatalytic activity. Photocatalyst recycling experiments proved that TiO_2 nanoparticle had a good stability, favoring its practical application.

Acknowledgements

This research did not receive any specific grant from funding agencies.

References

1) **Gaya, U. I. and Abdullah, A. H. (2008).** Heterogeneous photocatalytic degradation of organic contaminants over titanium dioxide: A review of fundamentals, progress and problems. J. Photochem. Photobiol., C., **9**:1–12.
2) **Herrmann, J.-M., Guillard, C. and Pichat, P. (1993).** Heterogeneous photocatalysis: an emerging technology for water treatment. Catal. Today, **17**:7-20.
3) **Herrmann, J. M. (1999).** Heterogeneous photocatalysis: fundamentals and applications to the removal of various types of aqueous pollutants. Catal.Today., **53**:115–129.
4) **Hoffmann, M. R., Martin, S. T., Choi, W. and Bahnemann, D. W. (1995).** Environmental Applications of Semiconductor Photocatalysis. Chem. Rev., **95**: 69-96.
5) **Linsebigler, A. L., Lu, G. and Yates, Jr., J. T. (1995).** Photocatalysis on TiO_2 Surfaces: Principles, Mechanisms, and Selected Results. Chem. Rev., **95**:735-758.
6) **Chen, X. and Mao, S. S. (2007).** Titanium Dioxide Nanomaterials: Synthesis, Properties, Modifications, and Applications. Chem. Rev., **107**:2891-2959.
7) **Fujishima, A. and Zhang, X. (2006).** Titanium dioxide photocatalysis: present situation and future approaches. C. R. Chim., **9**:750–760.
8) **Fujishima, A., Rao, T. N. and Tryk, D. A. (2000).** Titanium dioxide photocatalysis. J. Photochem. Photobiol., C. **1**:1–2.
9) **Ochiai, T. and Fujishima, A. (2012).** Photoelectrochemical properties of TiO_2 photocatalyst and its applications for environmental purification. J. Photochem. Photobiol., C., **13**:247–262.
10) **Nakata, K., Ochiai, T., Murakami, T. and Fujishima, A. (2012).** Photoenergy conversion with TiO_2 photocatalysis: New materials and recent Applications. Electrochim. Acta., **84**:103– 111.
11) **Tolosana-Moranchel, A., Casas, J. A., Carbajo, J., Faraldos, M. and Bahamonde, A. (2017).** Influence of TiO2 optical parameters in a slurry photocatalytic reactor: Kinetic modeling. Appl. Catal., B, **200**:164–173.

12) **Murcia, J. J., Ávila-Martínez, E. G., Rojasa, H., Navío, J. A. and Hidalgo, M. C. (2017).** Study of the E. coli elimination from urban wastewater over photocatalysts based on metallized TiO_2. Appl. Catal., B, **200**:469–476.

13) **Bergamonti, L., Alfieri, I., Lorenzi, A., Montenero, A., Predieri, G. I., Barone, G., Mazzoleni, P., Pasquale, S. and Lottici, P. P. (2013).** Nanocrystalline TiO_2 by sol–gel: Characterisation and photocatalytic activity on Modica and Comiso stones. Appl. Surf. Sci., **282**:165– 173.

14) **Radoici, M. B., vana, I., Jankovi, A., Despotovi, V. N., Soji, D. V., Savi, T. D., Saponji, Z. V., Abramovi, B. F. and Comor, M. I. (2013).** The role of surface defect sites of titania nanoparticles in the photocatalysis: Aging and modification. Appl. Catal. B., **138– 139**:122– 127.

15) **Tseng, T. K., Lin, Y. S., Chen, Y. J. and Chu, Hsin (2010).** A Review of Photocatalysts Prepared by Sol-Gel Method for VOCs Removal. Int. J. Mol. Sci., **11**:2336-2361.

16) **Loryuenyong, V., Angamnuaysiri, K., Sukcharoenpong, J. and Suwannasri, A. (2012).** Sol–gel derived mesoporous titania nanoparticles: Effects of calcinations temperature and alcoholic solvent on the photocatalytic behavior. Ceram. Int., **38**:2233–2237.

17) **Ismail, A. A. and Bahnemann, D. W. (2011).** Mesoporous titania photocatalysts: preparation, characterization and reaction mechanisms. J. Mater. Chem., **21**:11686.

18) **Venkatachalam, N., Palanichamy, M. and Murugesan, V. (2007).** Sol–gel preparation and characterization of nanosize TiO_2: Its photocatalytic performance. Mater. Chem. Phys., **104**:454–459.

19) **Lin, Y. S. and Deng, S. G. (1998).** Sol–gel preparation of nanostructured adsorbents. Stud. Surf. Sci. Catal., **120**:653-686.

20) **Abou-Gamra, Z. M. and Ahmed, M. A. (2016).** Synthesis of mesoporous TiO_2–curcumin nanoparticles for photocatalytic degradation of methylene blue dye. J. Photochem. Photobiol. B, **160**:134–141.

21) **Nuengmatca, P., Mahachai, R. and Chanthai, S. (2014).** Thermodynamic and Kinetic Study of the Intrinsic Adsorption Capacity of Graphene Oxide for Malachite Green Removal from Aqueous Solution. Orient. J. Chem., **30**:1463-1474.

22) **Dai, K., Chen, H., Peng, T., Ke, D. and Yi, H. (2007)**. Photocatalytic degradation of methyl orange in aqueous suspension of mesoporous titania nanoparticles. Chemosphere. **69**:1361–1367.

23) **Guetta, N. and Amar, H. A. (2005).** Photocatalytic oxidation of methyl orange in presence of titanium dioxide in aqueous suspension. Part I: Parametric study. Desalination, **185**:427–437.

24) **Tokode, O., Prabhu, R., Lawton, L. A. and Robertson, P. K. J. (2014).** The effect of pH on the photonic efficiency of the destruction of methyl orange under controlled periodic illumination with UV-LED sources. Chem. Eng. J., **246**:337–342.

25) **Blin, J-L., Stébé, M-J. and Roques-Carmes, T. (2012).** Use of ordered mesoporous titania with semi-crystalline framework as photocatalyst. Colloids Surf., A, **407**:177–185.

26) **Farzana, M. H. and Meenakshi, S. (2014).** Photo-decolorization and detoxification of toxic dyes using titaniumdioxide impregnated chitosan beads. Int. J. Biol. Macromol. **70**:420–426.